Pergamon

Int. J. Solids Structures Vol. 33, No. 4, pp. 469–482, 1996

0020–7683/96 $9.50 + .00

0020–7683(95)00050–X

IN-PLANE VIBRATION AND STABILITY OF SHALLOW CIRCULAR ARCHES SUBJECTED TO AXIAL FORCES

HIROYUKI MATSUNAGA
Department of Architecture, Setsunan University, 17-8, Ikeda-nakamachi, Neyagawa 572, Osaka, Japan

(*Received* 12 *August* 1994; *in revised form* 20 *February* 1995)

Abstract—Natural frequencies and buckling loads of a simply supported shallow circular arch with sufficiently small depth-to-radius of curvature ratio ($H/R \ll 1$) subjected to initial axial tensile and/or compressive forces are analysed. By using the method of power series expansion of displacement components, a set of fundamental dynamic equations of a one-dimensional higher-order arch theory for in-plane vibration problems of shallow circular arches is derived through Hamilton's principle. Several sets of truncated approximate theories which can take into account the effects of both shear deformations with depth changes and rotary inertia are applied to solve the eigenvalue problems of an elastic arch. Convergence properties of the natural frequency and the buckling load of simply supported shallow circular arches are examined in detail. The present approximate theories can predict the natural frequencies and buckling loads of shallow circular arches with small length-to-depth ratio L/H more accurately compared with previously published results.

1. INTRODUCTION

Although the vibration and stability problems of straight beams with shear deformations have been well established, the same problems have not been so well investigated for curved beams or arches. The arch theory may be extremely complicated with coupling between bending and axial deformation modes in the context of the three-dimensional theory of elasticity. As in the theories of straight beams, some simplifying assumptions have been made in describing the deformation of arches so as to reduce the problem to one-dimensional theory. The Euler–Bernoulli hypothesis of plane cross-sections remaining plane after deformation was introduced in the classical arch theory. In order approximately to account for both transverse shear deformation and rotary inertia effects, the Timoshenko-type arch theory can be derived by using a shear correction coefficient κ^2. This factor is introduced to correct the contradictory shear stress distribution over the cross-section of the arch and cannot be found within the assumption of the theory itself. Recently, a set of the fundamental equations for slightly curved laminated composite beams of shallow curvatures has been presented by Qatu (1992). For simply supported single-layer curved beams, both the bending and axial frequencies have been obtained. Although the effects of shear deformation and rotary inertia are neglected in the theory, these effects have been considered in the second theory (Qatu, 1993) which deals with moderately thick laminated composite curved beams. Only the bending frequencies for simply supported curved beams have been presented by taking into account the first order effects of shear deformation and rotary inertia. A comparison between the results obtained by using thin and moderately thick curved beam equations has been made.

The finite element method has been used extensively in the vibration problems of curved beams or arches. A study of the vibrations of elastic circular arches was presented by Wolf, Jr (1971), in which the effect of rotary inertia was included, but transverse shear deformations were neglected. By taking into account the effects of rotary inertia and transverse shear deformations, a Timoshenko beam finite element which includes planar rigid body motion capability was developed by Heppler (1992). It has been pointed out that these effects become important for quite short arches with small subtended angles. A strain-based curved beam finite element, using Timoshenko's deep-beam formulation in a

system of curvilinear coordinates, has been employed by Sabir *et al.* (1994) to analyse the natural frequencies of circular arches. By assuming a linear variation of curvature, constant circumferential direct strain and constant shear strain in the element, the effects of shear deformations on the free vibration problem of circular arches have been demonstrated.

In order to introduce the effects of transverse shear deformations with thickness changes and rotary inertia, refined higher-order theories of plates have been developed. As an extension of the classical thin plate theory, applicability and reliability of the two-dimensional higher-order theory have been clarified in detail through the numerical results of static boundary-value problems of an extremely thick plate (Matsunaga, 1986, 1992). Natural frequencies and buckling loads of thick plates subjected to in-plane forces have been analysed by using the two-dimensional higher-order plate theory (Matsunaga, 1994). It can be said that two-dimensional higher-order plate theories are very useful for the static and dynamic analyses of a thick plate as extended theories of the classical thin plate theory. The same can be said of curved beams or arches. However, higher-order theories of arches which take into account the complete effects of shear deformations and rotary inertia have not been investigated.

This paper presents a one-dimensional higher-order theory of shallow circular arches with small depth-to-radius of curvature ratio and small length-to-depth ratio which can take into account the effects of both shear deformations with depth changes and rotary inertia. Several sets of the governing equations of truncated approximate theories are applied to the analysis of in-plane free vibration and stability problems of a simply supported shallow circular arch subjected to axial forces. On the basis of the power series expansions of displacement components, a fundamental set of dynamic equations of a one-dimensional higher-order arch theory for in-plane vibration problems of shallow circular arches is derived through Hamilton's principle. Linear constitutive relations for an elastic arch of isotropic materials are also derived in terms of the expanded displacement components. The equations of motion of an arch subjected to initial axial forces are also expressed in terms of the displacement components. Following the Navier solution procedure, the displacement components are expanded into Fourier series that satisfy the simply supported boundary conditions. The natural frequency of an arch subjected to axial forces is obtained by solving the eigenvalue problem numerically and the buckling load is determined when the natural frequency vanishes. The convergence properties of the present numerical solutions are shown to be accurate for the natural frequencies and buckling loads with respect to the order of approximate theories. A comparison of the natural frequencies and buckling loads is also made with previously published results. The present results obtained by various sets of approximate theories are considered to be accurate enough for shallow circular arches with small length-to-depth ratio and can be regarded as the benchmark data of the problem. It is noticed that the one-dimensional higher-order arch theory in the present paper can predict the natural frequencies and buckling loads of such arches more accurately when compared with previously published results.

2. FUNDAMENTAL EQUATIONS OF KINEMATICS OF A SHALLOW CIRCULAR ARCH

Consider a shallow circular arch of arc length L as shown in Fig. 1, having a thin rectangular cross-section of depth H and width B which is assumed to be sufficiently small relative to the depth. The radius of curvature R of the arch is assumed to be sufficiently large relative to the depth (i.e. $H/R \ll 1$). A polar coordinate system (x, y, z) is defined on the central axis of the circular arch, where the x-axis is taken along the central axis with the y-axis in the width direction and the z-axis in the direction normal to the tangent to the central axis. Assuming that the deformations of the arch take place in the x–z plane, the dynamic displacement components of an arch in the x, y and z directions, respectively, can be expressed as

$$u \equiv u(x, z; t), \quad v \equiv v(x, z; t) = 0, \quad w \equiv w(x, z; t), \tag{1}$$

where t denotes time. The displacement components may be expanded into power series of the normal coordinate z as follows:

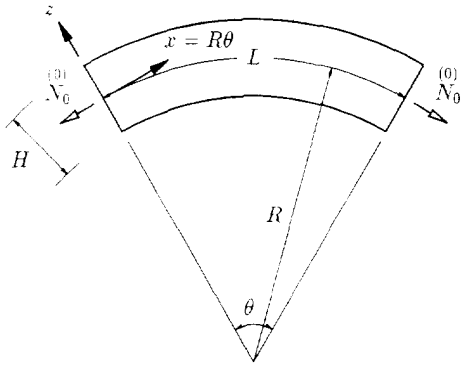

Fig. 1. Dimensions and coordinate system for an arch subjected to axial force.

$$u = \sum_{n=0}^{\chi} {}^{(n)}u\, z^n, \quad w = \sum_{n=0}^{\chi} {}^{(n)}w\, z^n, \tag{2}$$

where $n = 0, 1, 2, \ldots, \chi$.

Based on this expression of the displacement components, a set of the linear fundamental equations of a one-dimensional higher-order arch theory can be summarized as follows.

2.1. *Strain–displacement relations*

Strain components may be expanded as follows:

$$\varepsilon_{xx} = \sum_{n=0}^{\chi} {}^{(n)}\varepsilon_{xx}\, z^n, \quad \varepsilon_{zz} = \sum_{n=0}^{\chi} {}^{(n)}\varepsilon_{zz}\, z^n, \quad \gamma_{xz} = \gamma_{zx} = \sum_{n=0}^{\chi} {}^{(n)}\gamma_{xz}\, z^n \tag{3}$$

and strain–displacement relations can be written as (Yokoo and Matsunaga, 1974)

$${}^{(n)}\varepsilon_{xx} = {}^{(n)}u_{,x} - \frac{1}{R}{}^{(n)}w, \quad {}^{(n)}\varepsilon_{zz} = (n+1)\,{}^{(n+1)}w, \quad {}^{(n)}\gamma_{xz} = {}^{(n)}\gamma_{zx} = \frac{1}{2}\left\{(n+1)\,{}^{(n+1)}u - \frac{n-1}{R}{}^{(n)}u + {}^{(n)}w_{,x}\right\}, \tag{4}$$

where a comma denotes partial differentiation with respect to the coordinate subscripts that follow and an assumption $H/R \ll 1$ is used in the present derivation.

2.2. *Equations of motion and boundary conditions*

Under the assumption of plane strain or plane stress in the width direction, by introducing stress components σ_{xx}, $\tau_{xz} = \tau_{zx}$ and σ_{zz}, Hamilton's principle is applied to derive the equations of dynamic equilibrium and natural boundary conditions of an arch. In order to treat free vibration and stability problems of an arch subjected to axial stress σ^0_{xx} which distributes uniformly in the depth direction, additional work due to this stress which is assumed to remain unchanged during vibrating and or buckling is taken into consideration.

The principle for the present problems may be expressed for an arbitrary time interval t_1 to t_2 as follows:

$$\int_{t_1}^{t_2}\left[\int_V (\sigma_{xx}\delta\varepsilon_{xx} + 2\tau_{xz}\delta\gamma_{xz} + \sigma_{zz}\delta\varepsilon_{zz} - \rho\ddot{u}\delta u - \rho\ddot{w}\delta w)\,\mathrm{d}V + \int_I \sigma^0_{xx}({}^{(0)}u_{,x}\delta\,{}^{(0)}u_{,x} + {}^{(0)}w_{,x}\delta\,{}^{(0)}w_{,x})\,\mathrm{d}V - \int_S (\sigma^*_x\delta u + \sigma^*_z\delta w)\,\mathrm{d}S\right]\mathrm{d}t = 0, \tag{5}$$

where the overdot indicates partial differentiation with respect to time, ρ denotes the mass density, $\mathrm{d}V$ the volume element, $\mathrm{d}S$ the element of area of the external bounding surface

and σ_x^* and σ_z^* the prescribed components of the stress vector on the surface of an arch which are expressed in terms of the prescribed stress components as follows:

$$\sigma_x^* = n_x\sigma_{xx}^* + n_z\tau_{xz}^*, \quad \sigma_z^* = n_x\tau_{xz}^* + n_z\sigma_{zz}^*, \tag{6}$$

where n_x and n_z denote the components of the outward unit vector normal to the external bounding surface of the arch.

By performing the variation as indicated in eqn (5), the equations of motion are obtained as follows:

$$\begin{aligned}
&\delta\overset{(n)}{u}: \overset{(n)}{N}_{,x} - n\overset{(n-1)}{Q} + \frac{n-1}{R}\overset{(n)}{Q} + \overset{(n)}{p}_x = \rho\sum_{m=0}^{\infty} f(n+m+1)\overset{(m)}{\ddot{u}} \quad (\text{for } n \geqslant 1)\\
&\delta\overset{(0)}{u}: \overset{(0)}{N}_{,x} - \frac{1}{R}\overset{(0)}{Q} + (\overset{(0)}{N}_0\overset{(0)}{u}_{,x})_{,x} + \overset{(0)}{p}_x = \rho\sum_{m=0}^{\infty} f(m+1)\overset{(m)}{\ddot{u}}\\
&\delta\overset{(n)}{w}: \frac{1}{R}\overset{(n)}{N} + \overset{(n)}{Q}_{,x} - n\overset{(n-1)}{T} + \overset{(n)}{p}_z = \rho\sum_{m=0}^{\infty} f(n+m+1)\overset{(m)}{\ddot{w}} \quad (\text{for } n \geqslant 1)\\
&\delta\overset{(0)}{w}: \frac{1}{R}\overset{(0)}{N} + \overset{(0)}{Q}_{,x} + (\overset{(0)}{N}_0\overset{(0)}{w}_{,x})_{,x} + \overset{(0)}{p}_z = \rho\sum_{m=0}^{\infty} f(m+1)\overset{(m)}{\ddot{w}},
\end{aligned} \tag{7}$$

where $n, m = 0, 1, 2, \ldots, \infty$.

The stress resultants are defined as follows:

$$\overset{(0)}{N}_0 = H\sigma_{xx}^0, \quad \overset{(n)}{N} = \int_{-H/2}^{+H/2}\sigma_{xx}z^n\,dz, \quad \overset{(n)}{Q} = \int_{-H/2}^{+H/2}\tau_{xz}z^n\,dz, \quad \overset{(n)}{T} = \int_{-H/2}^{+H/2}\sigma_{zz}z^n\,dz. \tag{8}$$

Load terms measured per unit length of the central axis are expressed as

$$\overset{(n)}{p}_x = [\tau_{xz}^* z^n]_{-H/2}^{+H/2}, \quad \overset{(n)}{p}_z = [\sigma_{zz}^* z^n]_{-H/2}^{+H/2}, \tag{9}$$

where the stress components marked with an asterisk denote the prescribed quantities on the upper and lower surfaces of an arch and the following function is defined as

$$f(k) \equiv \int_{-H/2}^{+H/2} z^{k-1}\,dz = \frac{1}{k}\left(\frac{H}{2}\right)^k[1-(-1)^k] = \begin{cases} 0 & (k:\text{even}) \\ \dfrac{2}{k}\left(\dfrac{H}{2}\right)^k & (k:\text{odd}), \end{cases} \tag{10}$$

where k is an integer.

The equations of boundary conditions on the upper and lower surfaces are expressed as

$$\tau_{xz} = \tau_{xz}^*, \quad \sigma_{zz} = \sigma_{zz}^* \tag{11}$$

and at the ends on the central axis as follows:

$$\begin{aligned}
&\overset{(n)}{u} = \overset{(n)}{u}^* \quad \text{or} \quad \overset{(n)}{N} = \overset{(n)}{N}^*\\
&\overset{(n)}{w} = \overset{(n)}{w}^* \quad \text{or} \quad \overset{(n)}{Q} = \overset{(n)}{Q}^*,
\end{aligned} \tag{12}$$

where $n = 0, 1, 2, \ldots, \infty$ and the quantities marked with an asterisk denote quantities prescribed at the ends on the central axis of an arch.

2.3. *Constitutive relations*

For elastic and isotropic materials, the two-dimensional constitutive relations can be written as

$$\sigma_{xx} = 2\mu\varepsilon_{xx} + \bar{\lambda}(\varepsilon_{zz} + \varepsilon_{xx}), \quad \tau_{xz} = 2\mu\gamma_{xz}, \quad \sigma_{zz} = 2\mu\varepsilon_{zz} + \bar{\lambda}(\varepsilon_{xx} + \varepsilon_{zz}). \tag{13}$$

According to the assumption of plane strain or plane stress in the width direction, the coefficient $\bar{\lambda}$ is defined by

$$\bar{\lambda} = \begin{cases} \lambda & \text{(plane strain)} \\ \dfrac{2\mu\lambda}{2\mu+\lambda} & \text{(plane stress).} \end{cases} \tag{14}$$

where Lamé's constants μ and λ are defined by using Young's modulus E and Poisson's ratio ν as follows:

$$\mu \equiv \frac{E}{2(1+\nu)}, \quad \lambda \equiv \frac{\nu E}{(1+\nu)(1-2\nu)}. \tag{15}$$

2.4. *Stress resultants in terms of the expanded displacement components*

Stress resultants can be derived from eqns (8) and eqns (13) in terms of the expanded displacement components.

$$\begin{aligned}
\overset{(m)}{N} &= \sum_{n=0}^{\infty}\left[(2\mu+\bar{\lambda})\left(\overset{(n)}{u}_{,x} - \frac{1}{R}\overset{(n)}{w}\right) + \bar{\lambda}(m+1)\overset{(n+1)}{w}\right] f(n+m+1) \\
\overset{(m)}{Q} &= \sum_{n=0}^{\infty}\left[\mu\left\{(m+1)\overset{(n+1)}{u} - \frac{m-1}{R}\overset{(n)}{u} + \overset{(n)}{w}_{,x}\right\}\right] f(n+m+1) \\
\overset{(m)}{T} &= \sum_{n=0}^{\infty}\left[(2\mu+\bar{\lambda})(m+1)\overset{(n+1)}{w} - \bar{\lambda}\left(\overset{(n)}{u}_{,x} - \frac{1}{R}\overset{(n)}{w}\right)\right] f(n+m+1),
\end{aligned} \tag{16}$$

where $n, m = 0, 1, 2, \ldots, \infty$.

2.5. *Equations of motion in terms of the expanded displacement components*

The equations of motion can be expressed in terms of the expanded displacement components by using eqns (16) as

$$\begin{aligned}
\delta\overset{(m)}{u}: \sum_{n=0}^{\infty}\Bigg[\Bigg\{\Bigg[(2\mu+\bar{\lambda})\left(\overset{(n)}{u}_{,x} - \frac{1}{R}\overset{(n)}{w}\right) + \bar{\lambda}(m+1)\overset{(n+1)}{w}\Bigg], \\
+ \frac{n-1}{R}\mu\left[(m+1)\overset{(n+1)}{u} - \frac{m-1}{R}\overset{(n)}{u} + \overset{(n)}{w}_{,x}\right] - \rho\overset{(n)}{\ddot{u}}\Bigg\} f(n+m+1) \\
- n\mu\left[(m+1)\overset{(n+1)}{u} - \frac{m-1}{R}\overset{(n)}{u} + \overset{(n)}{w}_{,x}\right] f(n+m)\Bigg] + \overset{(m)}{p}_x = 0 \quad (\text{for } n \geqslant 1)
\end{aligned}$$

$$\begin{aligned}
\delta\overset{(0)}{u}: \sum_{m=0}^{\infty}\Bigg\{\Bigg[(2\mu+\bar{\lambda})\left(\overset{(m)}{u}_{,x} - \frac{1}{R}\overset{(m)}{w}\right) + \bar{\lambda}(m+1)\overset{(m+1)}{w}\Bigg], \\
- \frac{1}{R}\mu\left[(m+1)\overset{(m+1)}{u} - \frac{m-1}{R}\overset{(m)}{u} + \overset{(m)}{w}_{,x}\right] - \rho\overset{(m)}{\ddot{u}}\Bigg\} f(m+1) + (\overset{(0)}{N}_0\overset{(0)}{u}_{,x})_{,x} + \overset{(0)}{p}_x = 0
\end{aligned}$$

$$\overset{(n)}{\delta w}: \sum_{m=0}^{\infty}\left[\left\{\frac{1}{R}\left[(2\mu+\bar{\lambda})\left(\overset{(m)}{u}_{,x}-\frac{1}{R}\overset{(m)}{w}\right)+\bar{\lambda}(m+1)\overset{(m+1)}{w}\right]\right.\right.$$
$$\left.+\mu\left[(m+1)\overset{(m+1)}{u}-\frac{m-1}{R}\overset{(m)}{u}+\overset{(m)}{w}_{,x}\right]_{,x}-\rho\overset{(m)}{\ddot{w}}\right\}f(n+m+1)$$
$$\left.-n\left[(2\mu+\bar{\lambda})(m+1)\overset{(m-1)}{w}+\bar{\lambda}\left(\overset{(m)}{u}_{,x}-\frac{1}{R}\overset{(m)}{w}\right)\right]f(n+m)\right]+\overset{(n)}{p_z}=0 \quad (\text{for } n\geqslant 1)$$

$$\overset{(0)}{\delta w}: \sum_{m=0}^{\infty}\left\{\frac{1}{R}\left[(2\mu+\bar{\lambda})\left(\overset{(m)}{u}_{,x}-\frac{1}{R}\overset{(m)}{w}\right)+\bar{\lambda}(m+1)\overset{(m+1)}{w}\right]\right.$$
$$\left.+\mu\left[(m+1)\overset{(m+1)}{u}-\frac{m-1}{R}\overset{(m)}{u}+\overset{(m)}{w}_{,x}\right]_{,x}-\rho\overset{(m)}{\ddot{w}}\right\}f(m+1)+\overset{(0)}{(N_0}\overset{(0)}{w}_{,x})_{,x}+\overset{(0)}{p_z}=0. \quad (17)$$

2.6. M*th order approximate theory*

Since the fundamental equations mentioned above are complex, approximate theories of various orders may be considered for the present problem. A set of the following combination of displacement components for Mth ($M \geqslant 1$) order approximate equations is proposed.

$$u=\sum_{m=0}^{2M-1}\overset{(m)}{u}z^m, \quad w=\sum_{m=0}^{2M-2}\overset{(m)}{w}z^m, \quad (18)$$

where $m = 0, 1, 2, 3, \ldots$.

The total number of the unknown displacement components is $(4M-1)$. In the above cases of $M = 1$, an assumption of plane strains in the depth direction is inherently imposed. Another set of the governing equations of the lowest order approximate theory ($M = 1$†) is derived with the use of an assumption that the normal stress σ_{zz} is zero. This theory corresponds to the Timoshenko-type arch theory with the shear correction coefficient $\kappa^2 = 1$. The normal strain in the depth direction is obtained from the last equation in eqn (13) as

$$\varepsilon_{zz}=\frac{-\bar{\lambda}}{2\mu+\bar{\lambda}}\varepsilon_{xx}. \quad (19)$$

Under the assumption of plane state of stresses in the depth direction, the shear strain γ_{xz} must vanish through the depth of an arch and the lowest order approximate theory is reduced to the classical arch theory.

3. FOURIER SERIES SOLUTION FOR A SIMPLY SUPPORTED CIRCULAR ARCH

A simply supported circular arch of thin rectangular cross-section subjected to axial forces undergoing in-plane deformation is analysed for natural frequencies and buckling loads.

The simply supported boundary conditions (12) can be expressed at the x-constant points, $x = 0$ and $x = L$ as

$$\overset{(n)}{N}=0, \quad \overset{(n)}{w}=0. \quad (20)$$

For free vibration and buckling problems, load terms are set as follows:

$$\overset{(n)}{p_x}=\overset{(n)}{p_z}=0. \quad (21)$$

Since a circular arch is in a state of uniform stress, the axial forces are considered to be constant during vibration and/or buckling. Following the Navier solution procedure, displacement components that satisfy the equations of boundary conditions (20) may be expressed as

$$\overset{(n)}{u} = \sum_{r=1}^{\infty} \overset{(n)}{u_r} \cos\frac{r\pi X}{L} \cdot e^{i\omega t}, \quad \overset{(n)}{w} = \sum_{r=1}^{\infty} \overset{(n)}{w_r} \sin\frac{r\pi X}{L} \cdot e^{i\omega t}, \tag{22}$$

where the displacement mode number $r = 1, 2, 3, \ldots, \infty$, ω denotes the circular frequency and i the imaginary unit.

The equations of motion are rewritten in terms of the generalized displacement components $\overset{(n)}{u_r}$ and $\overset{(n)}{w_r}$. The dimensionless natural frequency and the buckling load or the initial axial force in the x direction for vibration problems are defined as follows:

$$\Omega = \omega H\sqrt{(\rho/G)}, \quad \Lambda = B\overset{(0)}{N_0}/P_c, \tag{23}$$

where G is the shear modulus and P_c is the minimum buckling load for the bending problem of a straight beam from the classical beam theory defined by

$$G = E/2(1+\nu), \quad P_c = \pi^2 EI/L^2, \quad I = BH^3/12. \tag{24}$$

4. EIGENVALUE PROBLEM FOR IN-PLANE VIBRATION AND STABILITY OF SHALLOW CIRCULAR ARCH

Equations (17) can be rewritten by collecting the coefficients for the generalized displacements of any fixed value r. The generalized displacement vector $\{\mathbf{U}\}$ for the Mth order approximate theory is expressed as

$$\{\mathbf{U}\}^{\mathrm{T}} = \left\{\overset{(0)}{u_r}, \ldots, \overset{(2M-1)}{u_r}; \overset{(0)}{w_r}, \ldots, \overset{(2M-2)}{w_r}\right\}. \tag{25}$$

For free vibration problems, the equations of motion can be expressed as the following eigenvalue problem:

$$([\mathbf{K}] - \Omega^2[\mathbf{M}])\{\mathbf{U}\} = 0. \tag{26}$$

where matrix [**K**] denotes the stiffness matrix which may contain the terms of the initial axial forces and matrix [**M**] is the mass matrix.

For stability problems, the natural frequency is set to zero and the stability equation can be expressed as the following eigenvalue problem:

$$([\mathbf{K}] + \Lambda[\mathbf{S}])\{\mathbf{U}\} = 0. \tag{27}$$

where matrix [**K**] denotes the stiffness matrix and matrix [**S**] is the geometric-stiffness matrix due to the axial force.

The power method is used to obtain the numerical solution of the eigenvalue problems. Although all the eigenvalues and eigenvectors can be computed by this method, the dominant eigenvalue which corresponds to the minimum natural frequency and/or the critical buckling load is much concerned.

Table 1(a). Convergence property of natural frequencies‡

L/H	L/R	Ω	CAT	TAT	$M = 1$†	$M = 2$	$M = 3$	$M = 4$
2	0.00	Ω_1	1.1485	0.8626	0.8875	0.8693	0.8689	←
		Ω_2	2.5328	2.5328	2.5328	2.5048	2.5024	←
	0.10	Ω_1	1.1478	0.8612	0.8861	0.8690	0.8685	←
		Ω_2	2.5344	2.5341	2.5341	2.5059	2.5034	←
	0.20	Ω_1	1.1456	0.8569	0.8817	0.8679	0.8673	←
		Ω_2	2.5393	2.5379	2.5379	2.5090	2.5065	←
	0.30	Ω_1	1.1420	0.8499	0.8745	0.8659	0.8653	←
		Ω_2	2.5473	2.5443	2.5443	2.5143	2.5118	←
	0.40	Ω_1	1.1370	0.8402	0.8645	0.8632	0.8625	←
		Ω_2	2.5584	2.5530	2.5530	2.5217	2.5190	←
5	0.00	Ω_1	0.1838	0.1727	0.1740	0.1730	←	←
		Ω_2	1.0131	1.0131	1.0131	1.0116	←	←
	0.25	Ω_1	0.1832	0.1710	0.1723	0.1724	←	←
		Ω_2	1.0164	1.0163	1.0163	1.0147	←	←
	0.50	Ω_1	0.1814	0.1661	0.1674	0.1708	←	←
		Ω_2	1.0263	1.0258	1.0258	1.0241	←	←
	0.75	Ω_1	0.1786	0.1582	0.1594	0.1681	←	←
		Ω_2	1.0425	1.0414	1.0414	1.0394	←	←
	1.00	Ω_1	0.1749	0.1477	0.1488	0.1641	←	←
		Ω_2	1.0647	1.0626	1.0626	1.0606	←	←

‡See Table 1(b).

5. NUMERICAL EXAMPLES AND RESULTS

5.1. *Numerical examples*

A simply supported shallow circular arch with small length-to-depth ratio L/H and sufficiently thin rectangular cross-sections subjected to initial axial tensile and/or compressive forces is analysed for the following parameters of the length-to-depth ratio

$$L/H = 1, 2, 4, 5, 10, 20. \tag{28}$$

Since the curvature parameter is assumed to be $H/R \ll 1$, the limit of this parameter is taken to be $H/R = 0.2$ (Qatu, 1993) and the length-to-radius of curvature ratio L/R is varied from 0.0 to 1.0 in the present numerical examples. Poisson's ratio is fixed at $\nu = 0.3$. All the numerical results are obtained for the case of plane stress in the width direction of an arch and are shown in the dimensionless quantities.

5.2. *Convergence property of solutions and comparison with previously published results*

Any arch theory is necessarily of an approximate character to provide a one-dimensional representation of an intrinsically three-dimensional phenomenon. In order to verify the accuracy of the present results, convergence properties of the numerical solutions according to the order of approximate theories are examined. It is noticed that the proper order of the present approximate theories may be estimated according to the level of L/H of the arch. Although the present sets of approximate theories can easily be applied to a circular arch with large L/H, higher orders of the expanded one-dimensional theories may be required to obtain reasonably accurate solutions for an arch with small L/H. Convergence properties of the first two natural frequencies of an arch without initial axial forces and the buckling loads of an arch subjected to axial compressive forces are examined in detail.

In Table 1, the first two natural frequencies Ω_1 and Ω_2 and the first two buckling loads Λ_1 and Λ_2 for the first displacement mode $r = 1$ are compared with the solutions obtained by the classical arch theory and the Timoshenko-type arch theory for several values of L/H and L/R. The lower natural frequency Ω_1 and buckling load Λ_1 are for predominantly bending modes with some shear deformation, whereas the upper frequency Ω_2 and buckling load Λ_2 are for predominantly axial modes. It is noticed that the present results for $M = 1$–5 converge accurately enough within the present order of approximate theories. In the following, only the numerical results for $M = 5$ are discussed, which is considered to be sufficient with respect to the accuracy of the solutions. In the first order approximate theory

Table 1(b). Convergence property of buckling loads

L/H	L/R	Λ	CAT	TAT	$M=1\dagger$	$M=2$	$M=3$	$M=4$	$M=5$
2	0.00	Λ_1	1.0000	0.6092	0.6516	0.5958	0.5939	0.5921	0.5912
		Λ_2	4.8634	4.8634	4.8634	4.1146	3.6344	3.4623	3.3758
	0.10	Λ_1	0.9987	0.6070	0.6492	0.5954	0.5934	0.5916	0.5906
		Λ_2	4.8696	4.8712	4.8714	4.1179	3.6373	3.4650	3.3785
	0.20	Λ_1	0.9949	0.6004	0.6422	0.5938	0.5918	0.5900	0.5889
		Λ_2	4.8882	4.8943	4.8952	4.1278	3.6459	3.4731	3.3869
	0.30	Λ_1	0.9887	0.5897	0.6305	0.5911	0.5891	0.5872	0.5862
		Λ_2	4.9191	4.9328	4.9348	4.1443	3.6604	3.4867	3.4008
	0.40	Λ_1	0.9801	0.5751	0.6147	0.5873	0.5853	0.5834	0.5823
		Λ_2	4.9622	4.9863	4.9897	4.1673	3.6806	3.5057	3.4203
5	0.00	Λ_1	1.0000	0.9069	0.9212	0.9021	0.9020	0.9019	←
		Λ_2	30.3964	30.3964	30.3964	29.4848	28.7171	28.4227	28.2679
	0.25	Λ_1	0.9935	0.8891	0.9031	0.8964	0.8963	0.8961	←
		Λ_2	30.5953	30.6124	30.6127	29.6657	28.8918	28.5949	28.4392
	0.50	Λ_1	0.9745	0.8378	0.8510	0.8793	0.8790	0.8789	←
		Λ_2	31.1918	31.2584	31.2599	30.2080	29.4159	29.1115	28.9531
	0.75	Λ_1	0.9444	0.7583	0.7701	0.8507	0.8503	0.8502	←
		Λ_2	32.1843	32.3291	32.3323	31.1119	30.2890	29.9722	29.8093
	1.00	Λ_1	0.9054	0.6584	0.6686	0.8105	0.8101	0.8100	←
		Λ_2	33.5707	33.8165	33.8220	32.3771	31.5108	31.1761	31.0069

‡CAT: classical arch theory; TAT. Timoshenko-type arch theory ($\kappa^2 = 5/6$); $M = 1\dagger$, plane stress in depth direction (Timoshenko-type arch theory : $\kappa^2 = 1$)

($M = 1\dagger$), since the normal stress σ_{zz} is made to be zero, the results correspond to those of the Timoshenko-type arch theory with the shear correction coefficient $\kappa^2 = 1$. For small L/H, although the convergence property of the second buckling load for the predominantly axial mode is not so good, the convergence properties of the other quantities are accurate enough within the present order of approximate theories. In the following tables and figures, except Figs 3(a,b), absolute values of the buckling loads are shown.

The first two natural frequencies of shallow circular arches with moderately small length-to-depth ratio $L/H = 20$ are compared directly with the previously published results (Qatu, 1992) in Table 2(a). The form of dimensionless natural frequencies in the table is different from that of the first equation in eqn (23), i.e. $\bar{\Omega}_1 = \omega L^2\sqrt{(12\rho/EH^2)}$, $\bar{\Omega}_2 = \omega L\sqrt{(\rho/E)}$. Since the effects of shear deformation and rotary inertia are neglected and only the stretching–bending coupling due to curvature has been considered in Qatu's results, slight differences of natural frequencies from the present results

Table 2(a). Comparison of the first two natural frequencies with previously published results : effects of the thickness parameter ($L/H = 20$)

		Displacement mode : r				
L/R	$\bar{\Omega}$‡	1	2	3	4	5
0.00	$\bar{\Omega}_{1Q}$	9.8696	39.478–	88.826–	157.91–	246.74–
	$\bar{\Omega}_{1M}$	9.8293	38.8485	85.7505	148.6440	225.3584
	$\bar{\Omega}_{2Q}$	3.1416	6.2832	9.4247	12.566–	15.708–
	$\bar{\Omega}_{2M}$	3.1413	6.2808	9.4168	12.5470	15.6694
0.20	$\bar{\Omega}_{1Q}$	9.8496	39.458–	88.806–	157.89–	246.72–
	$\bar{\Omega}_{1M}$	9.8094	38.8288	85.7313	148.6255	225.3405
	$\bar{\Omega}_{2Q}$	3.1480	6.2864	9.4269	12.568–	15.709–
	$\bar{\Omega}_{2M}$	3.1477	6.2840	9.4189	12.5486	15.6706
0.50	$\bar{\Omega}_{1Q}$	9.7466	39.353–	88.699–	157.78–	246.60–
	$\bar{\Omega}_{1M}$	9.7041	38.7256	85.6306	148.5279	225.2465
	$\bar{\Omega}_{2Q}$	3.1812	6.3032	9.4383	12.576–	15.716–
	$\bar{\Omega}_{2M}$	3.1808	6.3006	9.4299	12.5568	15.6770
1.00	$\bar{\Omega}_{1Q}$	9.4038	38.983–	88.321–	157.39–	246.21–
	$\bar{\Omega}_{1M}$	9.3184	38.3548	85.2698	148.1786	224.9102
	$\bar{\Omega}_{2Q}$	3.2972	6.3629	9.4786	12.607–	15.741–
	$\bar{\Omega}_{2M}$	3.2964	6.3595	9.4690	12.5859	15.7000

‡$\bar{\Omega}_{1Q}$ and $\bar{\Omega}_{2Q}$, Qatu's results (1992) : $\bar{\Omega}_{1M}$ and $\bar{\Omega}_{2M}$, present results ($M = 5$) ; dimensionless frequencies, $\bar{\Omega}_1 = \omega L^2\sqrt{(12\rho/EH^2)}$, $\bar{\Omega}_2 = \omega L\sqrt{(\rho/E)}$.

Table 2(b). Comparison of the first two natural frequencies with previously published results : effects of the curvature parameter ($L/R = 1.0$)

		Displacement mode : r				
L/H	$\bar{\Omega}_{1}^{\ddagger}$	1	2	3	4	5
5	$\bar{\Omega}_{1Q}$	8.0874	32.122 –	63.760 –	98.806 –	—
	$\bar{\Omega}_{1M}$	8.8119	31.9473	61.7087	94.1744	127.6434
10	$\bar{\Omega}_{1Q}$	8.3546	36.153 –	78.546 –	131.57 –	—
	$\bar{\Omega}_{1M}$	9.2083	36.6930	77.9959	128.9675	186.3153
20	$\bar{\Omega}_{1Q}$	8.4270	37.504 –	84.790 –	148.58 –	—
	$\bar{\Omega}_{1M}$	9.3184	38.3548	85.2698	148.1786	224.9102
50	$\bar{\Omega}_{1Q}$	8.4478	37.919 –	86.909 –	155.06 –	—
	$\bar{\Omega}_{1M}$	9.3502	38.8734	87.8083	155.7889	242.3119
100	$\bar{\Omega}_{1Q}$	8.4508	37.980 –	87.229 –	155.07 –	—
	$\bar{\Omega}_{1M}$	9.3547	38.9497	88.1948	157.0009	245.2352

‡$\bar{\Omega}_{1Q}$, Qatu's results (1993) ; $\bar{\Omega}_{1M}$, present results ($M = 5$) ; dimensionless frequencies, $\bar{\Omega}_{1} = \omega L^2\sqrt{(12\rho/EH^2)}$.

are noticed. For the case of larger length-to-depth ratio $L/H = 100$, the difference of natural frequencies becomes smaller.

In Table 2(b), a similar comparison of the lowest natural frequency Ω_1 of shallow circular arches with the largest length-to-radius of curvature ratio $L/R = 1.0$ is also made with Qatu's results (1993) which were obtained by using moderately thick deep beam theory. Although the difference between shallow and deep beam theories is small for higher frequencies, a considerable difference for the fundamental frequency ($r = 1$) is noticed. For shallower cases of $L/R \ll 1$, this difference in natural frequencies becomes smaller. It may be said that the effect of the curvature parameter L/R is much more than that of the thickness parameter L/H upon the fundamental frequency.

5.3. *Natural frequencies of shallow circular arches without axial forces*

The first two natural frequencies obtained by the present analysis are shown in Table 3 for all the values of L/H and the first three displacement modes. The results are obtained for $M = 5$ with sufficient numerical accuracy and can be regarded as the benchmark data of natural frequencies of shallow circular arches with small L/H. Natural frequencies increase monotonically with increasing number of displacement modes.

5.4. *Buckling loads of shallow circular arches subjected to axial forces*

For a simply supported arch with axial compressive force, Figs 2(a,b) show the variation of the buckling loads with respect to displacement modes. The lower curve with the open circle shows the buckling loads for a predominantly bending mode with some shear deformation, whereas the upper curve with the open square shows those for a predominantly axial mode. As shown in Figs 2(a,b), the buckling loads for a predominantly axial mode decrease monotonically from those for $r = 1$ and then increase slightly. The lower buckling loads for a predominantly bending mode increase within lower displacement modes but decrease with higher displacement modes.

The buckling loads for the first three displacement modes and a higher displacement mode $r = 500$ are also shown in Table 4 for all values of L/H. The results are obtained for $M = 5$ with sufficient numerical accuracy and can be regarded as the benchmark data of buckling loads of shallow circular arches with small L/H. It is seen that the first displacement mode gives the critical buckling load for large L/H. However, for small L/H the critical buckling load does not correspond to lower displacement modes but to higher ones (for instance, $r = 500$). For this feature, limit points of the length-to-depth ratio $L/H = 3.191$ to 2.980 according to the length-to-radius of curvature ratio $L/R = 0.0$ to 1.0 appear in the present examples. The buckling loads of shallow circular arches for higher displacement modes approach those of straight beams.

Table 3. The first two natural frequencies of a shallow circular arch

			Displacement mode : r						Displacement mode : r		
L/H	L/R	Ω	1	2	3	L/H	L/R	Ω	1	2	3
1	0.00	Ω_1	2.3791	5.4910	8.5122	5	0.00	Ω_1	0.1730	0.6021	1.1546
		Ω_2	4.4428	6.3092	8.8123			Ω_2	1.0116	2.0122	2.9792
	0.05	Ω_1	2.3790	5.4913	8.5127		0.25	Ω_1	0.1724	0.6017	1.1543
		Ω_2	4.4425	6.3091	8.8127			Ω_2	1.0147	2.0136	2.9799
	0.10	Ω_1	2.3785	5.4918	8.5132		0.50	Ω_1	0.1708	0.6003	1.1532
		Ω_2	4.4414	6.3087	8.8139			Ω_2	1.0240	2.0179	2.9821
	0.15	Ω_1	2.3777	5.4926	8.5139		0.75	Ω_1	0.1680	0.5980	1.1514
		Ω_2	4.4396	6.3082	8.8159			Ω_2	1.0394	2.0251	2.9858
	0.20	Ω_1	2.3766	5.4935	8.5147		1.00	Ω_1	0.1641	0.5948	1.1490
		Ω_2	4.4371	6.3074	8.8186			Ω_2	1.0606	2.0350	2.9909
2	0.00	Ω_1	0.8689	2.3791	3.9447	10	0.00	Ω_1	0.0452	0.1730	0.3651
		Ω_2	2.5024	4.4428	5.3022			Ω_2	0.5064	1.0116	1.5142
	0.10	Ω_1	0.8685	2.3790	3.9448		0.25	Ω_1	0.0451	0.1728	0.3649
		Ω_2	2.5034	4.4425	5.3019			Ω_2	0.5080	1.0124	1.5147
	0.20	Ω_1	0.8673	2.3785	3.9449		0.50	Ω_1	0.0446	0.1724	0.3646
		Ω_2	2.5065	4.4414	5.3009			Ω_2	0.5127	1.0147	1.5162
	0.30	Ω_1	0.8652	2.3777	3.9451		0.75	Ω_1	0.0439	0.1718	0.3639
		Ω_2	2.5118	4.4396	5.2992			Ω_2	0.5205	1.0186	1.5187
	0.40	Ω_1	0.8624	2.3766	3.9453		1.00	Ω_1	0.0429	0.1708	0.3631
		Ω_2	2.5190	4.4371	5.2969			Ω_2	0.5313	1.0240	1.5222
4	0.00	Ω_1	0.2622	0.8689	1.6042	20	0.00	Ω_1	0.0114	0.0452	0.0998
		Ω_2	1.2633	2.5024	3.6443			Ω_2	0.2533	0.5064	0.7592
	0.20	Ω_1	0.2617	0.8685	1.6039		0.25	Ω_1	0.0114	0.0452	0.0998
		Ω_2	1.2658	2.5034	3.6446			Ω_2	0.2541	0.5068	0.7595
	0.40	Ω_1	0.2602	0.8673	1.6031		0.50	Ω_1	0.0113	0.0451	0.0996
		Ω_2	1.2732	2.5065	3.6455			Ω_2	0.2564	0.5080	0.7603
	0.60	Ω_1	0.2575	0.8652	1.6017		0.75	Ω_1	0.0111	0.0449	0.0995
		Ω_2	1.2854	2.5118	3.6469			Ω_2	0.2604	0.5100	0.7616
	0.80	Ω_1	0.2537	0.8624	1.5998		1.00	Ω_1	0.0108	0.0446	0.0992
		Ω_2	1.3023	2.5190	3.6489			Ω_2	0.2658	0.5127	0.7634

Table 4. The first two buckling loads of a shallow circular arch

			Displacement mode : r						Displacement mode : r			
L/H	L/R	Λ	1	2	3	500	L/H	L/R	Λ	1	2	3	500
1	0.00	Λ_1	0.2517	0.2348	0.1808	0.0772	5	0.00	Λ_1	0.9018	2.7789	4.4881	1.9422
		Λ_2	0.5086	0.3183	0.2655	0.2206			Λ_2	28.2679	23.5599	18.8480	5.5106
	0.05	Λ_1	0.2517	0.2347	0.1808	0.0772		0.25	Λ_1	0.8961	2.7746	4.4854	1.9422
		Λ_2	0.5087	0.3182	0.2655	0.2206			Λ_2	28.4392	23.5921	18.8581	5.5106
	0.10	Λ_1	0.2516	0.2347	0.1808	0.0772		0.50	Λ_1	0.8789	2.7618	4.4773	1.9422
		Λ_2	0.5088	0.3182	0.2654	0.2206			Λ_2	28.9531	23.6888	18.8883	5.5106
	0.15	Λ_1	0.2514	0.2346	0.1808	0.0772		0.75	Λ_1	0.8502	2.7404	4.4636	1.9422
		Λ_2	0.5092	0.3181	0.2653	0.2206			Λ_2	29.8093	23.8500	18.9388	5.5106
	0.20	Λ_1	0.2511	0.2345	0.1808	0.0772		1.00	Λ_1	0.8099	2.7104	4.4444	1.9422
		Λ_2	0.5112	0.3190	0.2658	0.2206			Λ_2	31.0069	24.0758	19.0096	5.5106
2	0.00	Λ_1	0.5912	1.0069	1.0414	0.3092	10	0.00	Λ_1	0.9736	3.6073	7.2239	7.8886
		Λ_2	3.3758	2.0344	1.5048	0.8823			Λ_2	119.3187	113.0715	104.2018	21.9992
	0.10	Λ_1	0.5906	1.0068	1.0413	0.3092		0.25	Λ_1	0.9674	3.6015	7.2189	7.8885
		Λ_2	3.3785	2.0346	1.5048	0.8823			Λ_2	120.0656	113.2429	104.2688	21.9992
	0.20	Λ_1	0.5889	1.0063	1.0410	0.3092		0.50	Λ_1	0.9488	3.5843	7.2037	7.8885
		Λ_2	3.3869	2.0354	1.5047	0.8823			Λ_2	122.3062	113.7569	104.4697	21.9992
	0.30	Λ_1	0.5862	1.0055	1.0406	0.3092		0.75	Λ_1	0.9179	3.5557	7.1784	7.8884
		Λ_2	3.4008	2.0366	1.5047	0.8823			Λ_2	126.0398	114.6136	104.8045	21.9992
	0.40	Λ_1	0.5823	1.0044	1.0399	0.3092		1.00	Λ_1	0.8747	3.5155	7.1429	7.8884
		Λ_2	3.4203	2.0384	1.5047	0.8823			Λ_2	131.2652	115.8124	105.2733	21.9992
4	0.00	Λ_1	0.8544	2.3646	3.4613	1.2404	20	0.00	Λ_1	0.9933	3.8942	8.4813	32.8711
		Λ_2	17.4185	13.5031	10.2537	3.5279			Λ_2	484.0376	477.2748	466.4784	87.7299
	0.20	Λ_1	0.8510	2.3624	3.4602	1.2404		0.25	Λ_1	0.9870	3.8881	8.4753	32.8709
		Λ_2	17.4846	13.5142	10.2568	3.5279			Λ_2	487.0938	478.0217	466.7983	87.7299
	0.40	Λ_1	0.8405	2.3558	3.4567	1.2404		0.50	Λ_1	0.9681	3.8695	8.4573	32.8706
		Λ_2	17.6829	13.5475	10.2662	3.5279			Λ_2	496.2623	480.2625	467.7584	87.7299
	0.60	Λ_1	0.8232	2.3447	3.4508	4.0221		0.75	Λ_1	0.9366	3.8386	8.4274	32.8704
		Λ_2	18.0132	13.6032	10.2817	3.5279			Λ_2	511.5424	483.9969	469.3584	87.7298
	0.80	Λ_1	0.7988	2.3291	3.4424	1.2404		1.00	Λ_1	0.8926	3.7954	8.3854	32.8703
		Λ_2	18.4755	13.6812	10.3036	3.5279			Λ_2	532.9327	489.2248	471.5982	87.7298

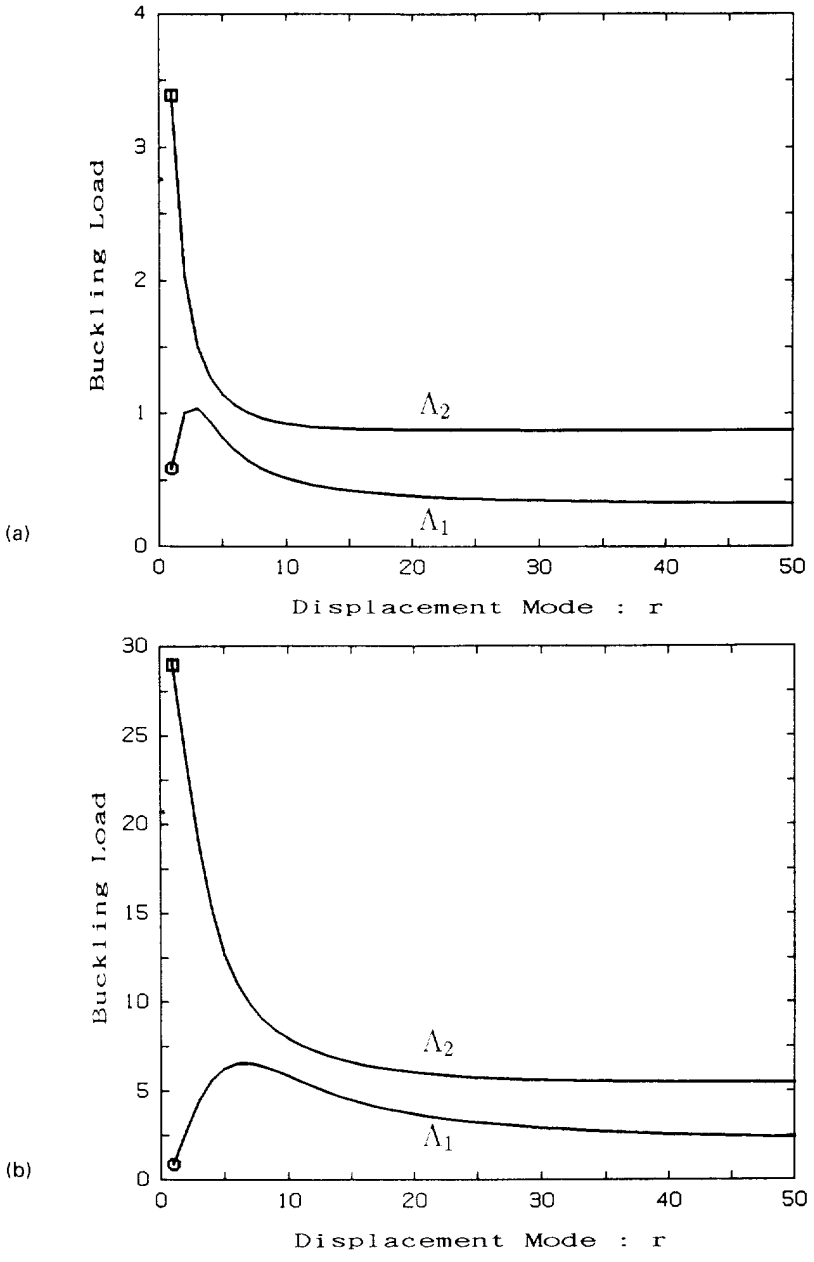

Fig. 2. Variation of buckling loads with respect to displacement mode : (a) $L/R = 0.2$, $L/H = 2$; (b) $L/R = 0.5$, $L/H = 5$.

5.5. *Natural frequencies of shallow circular arches subjected to initial axial forces*

The first two natural frequencies of shallow circular arches subjected to axial forces are plotted with respect to the initial axial forces in Figs 3(a,b). The figures show the effects of initial axial forces on the frequency curves for $r = 1$. When the natural frequencies go to zero, the initial axial forces reduce to the buckling loads of the arch.

6. DISCUSSION AND CONCLUSIONS

Beyond the limits of applicability of the existing arch theories, various orders of the expanded approximate theories have been applied to analyse the in-plane vibration and stability problems of a simply supported shallow circular arch with small L/H and sufficiently small H/R subjected to axial force.

The following conclusions may be drawn from the present analysis.

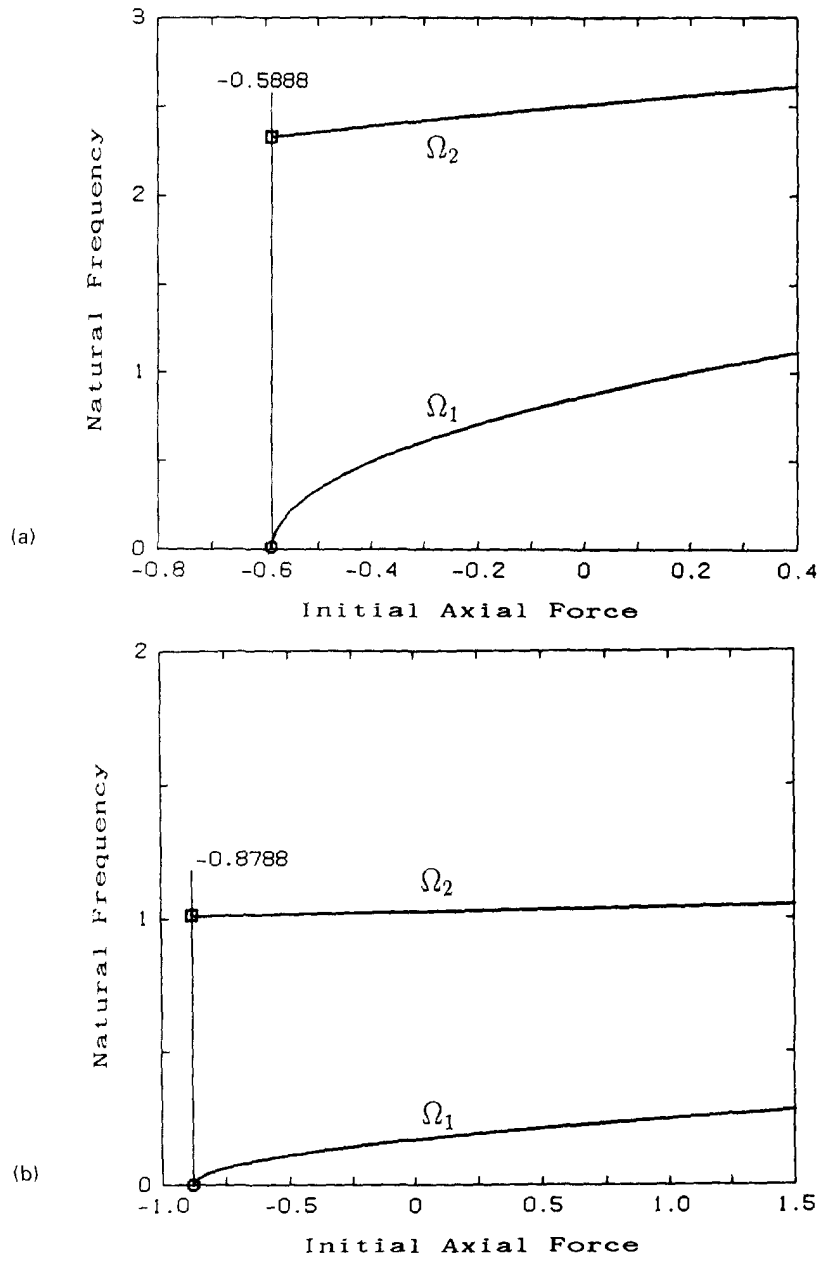

Fig. 3. First two natural frequencies for the first displacement mode ($r = 1$) vs initial axial force curves: (a) $L/R = 0.2$, $L/H = 2$; (b) $L/R = 0.5$, $L/H = 5$.

(1) In order to verify the accuracy of the present results, convergence properties of the numerical solutions according to the order of approximate theories are examined. Convergence properties of the first two natural frequencies and buckling loads for a simply supported shallow circular arch without axial force are examined in detail. An estimation of the approximate order of the governing equations may be concluded according to L/H of the arch. The present results obtained for $M = 5$ are considered to be accurate enough for arches with small L/H and can be regarded as the benchmark data of the problem.

It is found that the one-dimensional higher-order arch theory in the present paper can predict the natural frequencies and buckling loads of a shallow circular arch with small L/H and sufficiently small H/R more accurately when compared with previously published results.

(2) The first two natural frequencies of a simply supported shallow circular arch subjected to axial tensile and/or compressive forces have been obtained for all values of

L/H and several displacement modes. The first two natural frequencies of shallow circular arches subjected to axial forces are also plotted against the initial axial forces for the first displacement mode. When the natural frequencies go to zero, the initial axial forces reduce to the buckling loads of the arch.

For arches with the length-to-depth ratio L/H larger than a specific value of about 3.19, the critical buckling load appears at the first displacement mode $r = 1$. However, for arches with smaller L/H, lower buckling loads appear at higher displacement modes.

(3) The present one-dimensional approximate theories may require a larger value of M for shallow arches with smaller values of L/H to ensure the numerical accuracy of the results. For the present range of L/H, reasonably accurate numerical solutions are obtained for $M = 2$–5. It can be said that the present one-dimensional higher-order arch theory, which can take into account the effects of both shear deformations with depth changes and rotary inertia, is very effective for the in-plane vibration and stability analyses of a shallow circular arch as an extended theory of the Timoshenko-type arch theory and the classical arch theory.

REFERENCES

Heppler, G. R. (1992). An element for studying the vibration of unrestrained curved Timoshenko beams. *J. Sound Vibr.* **158,** 387–404.

Matsunaga, H. (1986). On the analysis of displacement and stress distributions of a thick elastic plate by two-dimensional higher order theory. *Trans A.I.J.* **367,** 48–58 (in Japanese).

Matsunaga, H. (1992). The application of a two-dimensional higher-order theory for the analysis of a thick elastic plate. *Comput. Structures* **45,** 633–648.

Matsunaga, H. (1994). Free vibration and stability of thick elastic plates subjected to in-plane forces. *Int. J. Solids Structures* **31,** 3113–3124.

Qatu, M. S. (1992). In-plane vibration of slightly curved laminated composite beams. *J. Sound Vibr.* **159,** 327–338.

Qatu, M. S. (1993). Theories and analyses of thin and moderately thick laminated composite curved beams. *Int. J. Solids Structures* **30,** 2743–2756.

Sabir, A. B., Djoudi, M. S. and Sfendji, A. (1994). The effects of shear deformation of circular arches by the finite element method. *Thin-Walled Structures* **18,** 47–66.

Wolf, J. A., Jr (1971). Natural frequencies of circular arches. *ASCE. J. Struct. Div.* **97,** 2337–2349.

Yokoo, Y. and Matsunaga, H. (1974). A general nonlinear theory of elastic shells. *Int. J. Solids Structures* **10,** 261–274.